IEICE Electronics Express, Vol.xx, No.xx, xx-xx

LETTER

Design of an integrated temperature and humidity sensor based on high dynamic range utilization rate ADC

Honghao Wu[1,3], Wenchang Li[1,2], Jian Liu[1,3] and Tianyi Zhang[1]

Abstract An integrated sensor for temperature (Temp) and humidity (RH) measurement is designed. The temperature and humidity (T/H) sensing probe are combined with one first-order discrete-time Σ-Δ analog-to-digital converter (ADC). Also, a new ample architecture of ADC is proposed, ADC selects a reasonable reference voltage according to varied range of T/H signals. Therefore, the dynamic range utilization rate of ADC is improved. The proposed sensor is designed and fabricated in 0.153μm CMOS technology. The experimental results show that the T/H sensor achieves a −0.9~0.6% RH measurement accuracy in the humidity range of 10~90% RH, and ±0.4°C temperature measurement accuracy in the temperature range of −40~120°C.
key words: Temperature, humidity, sensor, integrated circuits, ADC
Classification: Integrated circuits

1. Introduction

Temperature and humidity measurement are generally corelated and used as important parameters to represent fundamental status for environment or climate monitoring in fields like industrial control, material storage and manufacture, and ecological management [1, 2, 3, 4, 5]. With the development of the Internet of Things, portable devices and semiconductor fabrication technology, integrating multiple sensors into a single chip is one of the main directions. For this reason, integrated temperature and humidity (T/H) sensor chip has become a research hotspot in recent years.

In temperature measurement, bipolar junction transistor (BJT) based temperature sensor is the most widely used because it can achieve high accuracy over a wide temperature range [6, 7, 8, 9, 10] compared to resistor [11, 12] or MOS [13, 14, 15] based temperature sensors. In a variety of humidity sensing probes materials [16, 17, 18, 19, 20], polyimide has attracted more attention due to its compatibility with CMOS process. This design chooses BJT and polyimide to measure temperature and humidity respectively.

Considering temperature and humidity are both slowly variable physical quantities, moreover, both BJT and polyimide reflect temperature and humidity changes through voltage, a discrete-time ΣΔ ADC based on charge integration principle is more suitable for readout circuit [21, 22]. For multi-sensor chips, the types and ranges of analog signals corresponding to different physical quantities may be different, so it is crucial to match these signals reasonably with the dynamic range of ADC, otherwise the accuracy of the sensor will be reduced [23].

In view of the above problems, an integrated T/H sensor is designed. T/H sensing probe is integrated with first-order discrete-time ΣΔ ADC. Also, a new sample structure is proposed, ADC will select a reasonable reference voltage based on the different variation range of T/H signals, which improves the dynamic range utilization rate of ADC so sensor can achieve high precision measurement.

2. Principle of temperature and humidity sensing

2.1 Principle of humidity sensing

When polyimide absorbs water molecules, its dielectric parameter changes. Using this property, it is possible to make a plate capacitor using polyimide as a medium to measure humidity. The commonly used polyimide humidity sensitive probe with finger structure is shown in Fig. 1.

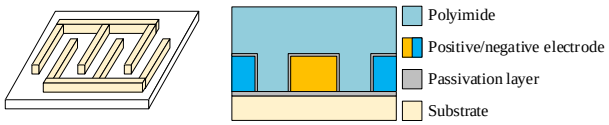

Fig. 1 Architecture of the humidity sensor probe

The metal fingers act as electrodes, and the polyimide above them needs to be exposed to air. The capacitance between the metal electrodes varies with humidity. The humidity of the current environment can be determined by measuring the capacitance value. The typical value of the humidity sensitive probe used in this paper is about

[1] Institute of Semiconductors, Chinese Academy of Sciences, Beijing 100083, China
[2] School of Microelectronics, University of Chinese Academy of Sciences, Beijing 100049, China
[3] College of Materials Science and Opto-Electronic Technology, University of Chinese Academy of Sciences, Beijing 100049, China
a) whh19@semi.ac.cn

DOI: 10.1587/elex.20.20230164
Received April 10, 2023
Accepted June 13, 2023
Publicized June 21, 2023

2.1pF, and the capacitor sensibility to humidity is about 4fF/%RH.

2.2 Principle of temperature sensing

When the emitter of a BJT is forward-biased through a current source, as shown in Fig. 2. V_{BE} can be expressed as:

$$V_{BE} = \frac{kT}{q}\ln\left(\frac{I_C}{I_S}\right) \quad (1)$$

Where q the electron charge (1.6×10^{-19} coulombs), k the Boltzmann constant, T is the Kelvin temperature, I_S the saturation current. V_{BE} has a negative temperature characteristic, with a temperature coefficient of about −2 mV/°C, and a slight nonlinearity. Therefore, ΔV_{BE}, the base-emitter voltage difference between two BJTs, is usually used to measure temperature [24, 25].

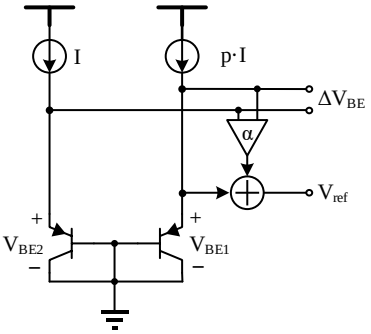

Fig. 2 Principle of temperature sensing based on BJT

Two identical BJTs are biased at current I and p·I, where p is an integer. If the BJT current gain is large enough, ΔV_{BE} can be expressed as

$$\Delta V_{BE} = \frac{kT}{q}\ln(p) \quad (2)$$

It can be seen that ΔV_{BE} is linearly and positively correlated with temperature. It is not affected by I_S, and has good linearity, with a temperature coefficient of about several hundred μV/°C. A temperature independent voltage, i.e. bandgap reference voltage, can be generated by using V_{BE} and $\alpha\Delta V_{BE}$ (α makes the temperature coefficients of V_{BE} and $\alpha\Delta V_{BE}$ consistent).

3. Proposed architecture

Fig. 3 (a) shows the traditional architecture [3]. The humidity sensing capacitor C_{RH} and BJT core convert humidity and temperature change into V_{RH} and $\alpha\Delta V_{BE}$, respectively. The output voltage V_{REF} of BJT core serves as the reference voltage of the ADC.

The temperature and humidity related outputs of traditional structures can be expressed as u_T = $\alpha\Delta V_{BE}/V_{REF}$ and u_{RH} = V_{RH}/V_{REF}, respectively. Taking temperature as an example, the variation interval of $\alpha\Delta V_{BE}$ in the temperature measurement range only accounts for about 30% of V_{REF} [26], which is only 30% of the ADC dynamic range is used, so at least 16 bits ADC is needed to achieve a resolution of 0.01°C. Such a ADC performance increases circuit design costs. The variation range of V_{RH} is also difficult to cover most of the dynamic range of ADC [27].

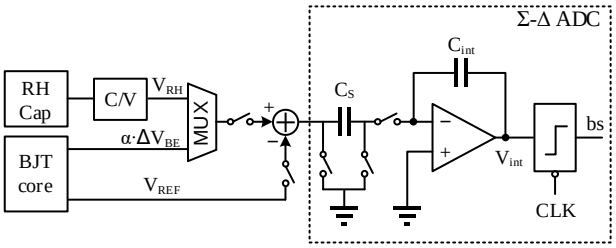

(a) Traditional structure

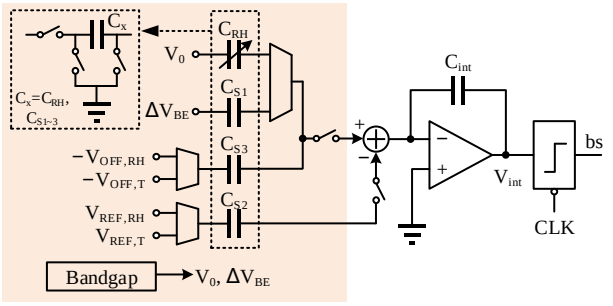

(b) Proposed structure

Fig. 3 Architecture of the proposed temperature and humidity sensor

In order to improve ADC dynamic range utilization, a new sample structure is proposed in this paper as shown in Fig. 3 (b), which introduces multiple sampling capacitors (C_{S1}~C_{S3}). Taking humidity measurement as an example, the output of ADC u_{RH} can be expressed as:

$$u_{RH} = \frac{C_{RH} - aC_{S3}}{bC_{S2}},\quad a = \frac{V_{OFF,RH}}{V_0}, b = \frac{V_{REF,RH}}{V_0} \quad (3)$$

V_0, $V_{OFF,RH}$, $V_{REF,RH}$ are reference voltage (RH in the subscript means humidity measurement, T means temperature measurement), aC_{S3} can be used as the offset capacitor C_{OFF} and bC_{S2} as the reference capacitor C_{REF}. By appropriately setting the values of C_{OFF} and C_{REF}, the dynamic range of ADC can be maximized, as shown in Fig. 4.

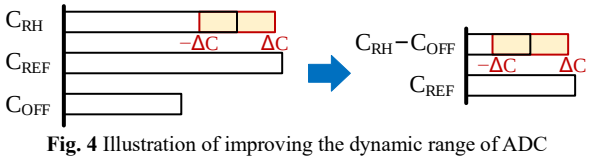

Fig. 4 Illustration of improving the dynamic range of ADC

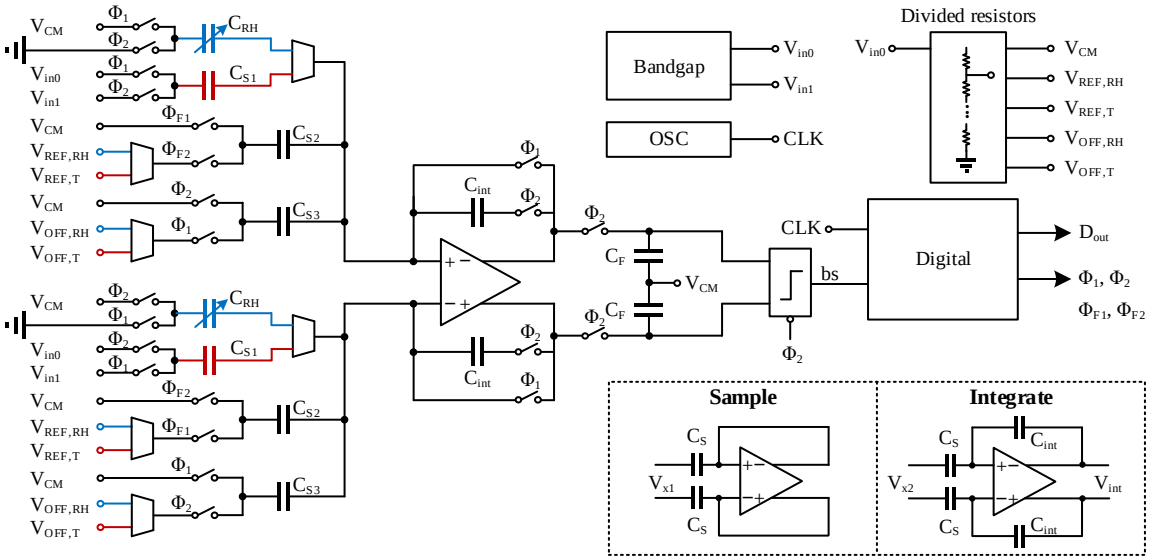

Fig. 5 Circuit diagram of the proposed temperature and humidity sensor

Compared with the humidity sensitive capacitor C_{RH}, the humidity sensitive capacitance value ΔC is much smaller. The dynamic range of the ADC for humidity measurement is only $2\Delta C/C_{RH}$. If appropriate C_{OFF} is selected, $2\Delta C$ can be closer to C_{REF}, thus improving the dynamic range utilization of the ADC. Similar results can be obtained from the analysis of temperature measurements.

4. Circuit design and implementation

This section will introduce the circuit design and implementation of the proposed integrated T/H sensor in detail. The overall circuit is shown in Fig. 5.

4.1 Bandgap reference

The bandgap reference is shown in Fig. 6. The current flowing through the transistor Q1 to Q3 is the same. The area ratio of the BJT Q1 and Q2 is 1:10. V_{in0} can be expressed as:

$$V_{in0} = V_{BE} + \frac{R_2 + R_3}{R_1}\Delta V_{BE} \tag{4}$$

By adjusting resistors R_1, R_2 and R_3, V_{in0} can be used as the bandgap reference voltage, and the common-mode voltages V_{CM}, $V_{REF,RH}$, $V_{REF,T}$, $V_{OFF,RH}$ and $V_{OFF,T}$ can be determined by the divided resistors network, as shown in Fig. 5. $V_{in0}-V_{in1} = (R_2/R_1)\cdot\Delta V_{BE}$, as the temperature sensing voltage.

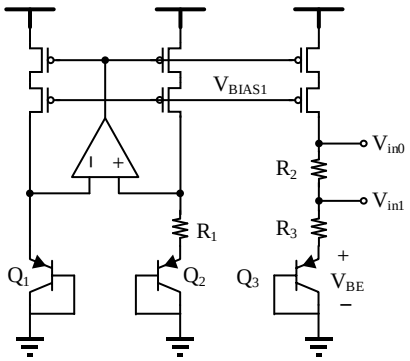

Fig. 6 Circuit diagram of the bandgap

4.2 First order ΣΔ ADC

The working process of discrete-time ΣΔ ADC can be divided into two steps: sample and integrate [28]. Its equivalent circuit is shown in Fig. 5, where the sampling capacitor can be C_{RH} and C_{S1}~C_{S3}. The integrated voltage V_{int} can be expressed as:

$$V_{int} = \frac{C_S}{C_{int}}\left(V_{x1} - V_{x2}\right) \tag{5}$$

V_{x1} and V_{x2} are input voltages of sampling phase and integration phase, respectively. V_{int} is sampled by C_F during integrate phase, digital code stream bs is generated through comparator, D_{out} is obtained by digital processing circuit. The digital part also generates feedback control timing Φ_{F1} and Φ_{F2} according to the state of bs.

The operational amplifier dominates performance of ΣΔ ADC. In this design, the folded-cascode structure is adopted [29], which can effectively increase the DC gain, the gain of the operational amplifier is about 102dB.

The comparator is edge-triggered, when Φ_2 is high, the

circuit does not work. When Φ_2 changes from high to low, the comparator starts working outputs rail to rail voltage based on the difference between the difference input signals V_P and V_M.

The output spectrum of ADC is shown in Fig. 7, the ADC achieves 87.2dB SNDR and 14.2 bits ENOB under 1024 times OSR.

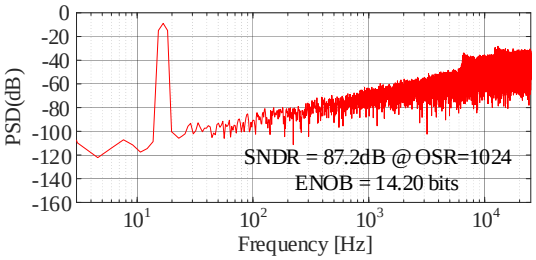

Fig. 7 Output spectrum of ADC

4.3 Conversion result

According to the analysis in section 3, the ADC output u_{RH} during humidity measurement can be obtained as:

$$u_{RH} = \frac{C_{RH} + mC_{S2} - nC_{S3}}{2mC_{S2}}$$
$$m = \frac{V_{CM} - V_{REF,RH}}{V_{CM}}, n = \frac{V_{CM} - V_{OFF,RH}}{V_{CM}} \quad (6)$$

In Eq. (6), mC_{S2}-nC_{S3} corresponds to the bias capacitor and $2mC_{S2}$ corresponds to the reference capacitor. In this design, the values of m and n are 0.1 and 0.4, C_{S2} and C_{S3} are 3.25pF and 5.2pF respectively, the capacitance variation range of C_{RH} is about 1.8~2.2pF in the range of 0~100% RH humidity. Thus, the dynamic range utilization of the ADC is about 62%. Similarly, the ADC output u_T during temperature measurement is

$$u_T = \frac{wC_{S1} + eC_{S2} - rC_{S3}}{2eC_{S2}}$$
$$w = \frac{V_{in0} - V_{in1}}{V_{CM}}, e = \frac{V_{CM} - V_{REF,T}}{V_{CM}}, r = \frac{V_{CM} - V_{OFF,T}}{V_{CM}} \quad (7)$$

In Eq. (7), w contains the temperature information, and varies from 0.031 to 0.064 in the range of −40 ℃ to 120℃. The values of e and r are 0.14 and 0.24, respectively, C_{S1} is 26pF. Thus, the dynamic range utilization of the ADC is about 90% during temperature measurement. It can be seen that ADC has a higher dynamic range utilization in the integrated T/H sensor structure proposed in this paper.

5. Experience results

The integrated T/H sensor is realized in 0.153μm CMOS process. The chip uses a ceramic package and an open window is made to expose the humidity sensitive capacitor to the air. The opening position corresponds to the humidity sensitive capacitor. The packaged integrated T/H sensor is shown in Fig. 8.

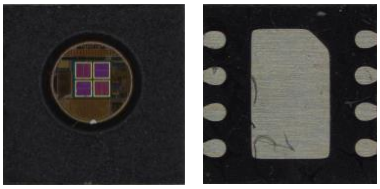

Fig. 8 Chip package of the proposed sensor

The chip test equipment is shown in Fig. 9, including temperature chamber, humidity generator, test board and other related instruments. During humidity test, the chip and high-precision humidity sensitive probe are put into the humidity generator at the same time, the high-precision humidity sensitive probe is used as the ambient humidity reference. During temperature test, the chip and the high-precision platinum resistor are put into the temperature chamber at the same time, the high-precision platinum resistor is used as the reference ambient temperature. The humidity and temperature measurement ranges from 10 to 90% RH and −40 to 120 ℃, respectively.

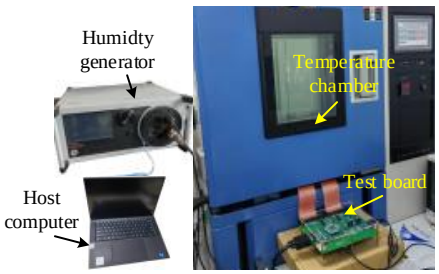

Fig. 9 Experiment setup

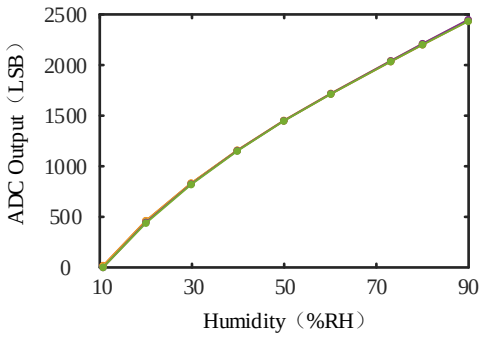

Fig. 10 Relationship between the ADC output and humidity

ADC outputs of different chips in different humidity environments are shown in Fig. 10. It can be seen that the ADC output in the range of 10~90% RH is 2500 LSB, i.e. 1 LSB corresponds to 0.03%RH. The chip behaves linearity together with a slight quadratic characteristic in the whole range of humidity. Therefore, the corresponding relationship between ADC output and

actual ambient humidity can be calculated as

$$RH_{out} = c_1 + c_2 D_{out,RH} + c_3 D_{out,RH}^2 \quad (8)$$

Where, RH_{out} is the measured humidity of the chip, $D_{out,RH}$ is the ADC output during humidity measurement, and c_1~c_3 is the fitting coefficient.

According to Eq. (8), c_1~c_3 could be obtained after fitting the chip output, so the actual measured humidity value of the chip can be calculated and compared with the high-precision humidity sensor to determine the humidity measurement error, as shown in Fig. 11. It can be seen that the humidity measurement accuracy of the chip is −0.9~0.6% RH in the humidity range of 10~90% RH.

ADC outputs of different chips under different temperature environments is shown in Fig. 12. In the range of -40℃ to 120℃, the ADC output is about 16,000 LSB, i.e. 1 LSB corresponds to 0.01℃. The chip temperature characteristic shows good linearity. The corresponding relationship between ADC output and actual ambient temperature can be calculated as following

$$T_{out} = d_1 + d_2 D_{out,T} \quad (9)$$

Where T_{out} is the measured temperature of the chip; $D_{out,T}$ is the output of ADC during temperature measurement; d_1, d_2 are the fitting coefficients.

Similar to the calculation method of humidity measurement error, according to Eq. (9), the temperature measurement error can be obtained, as shown in Fig. 13. It can be seen that the temperature measurement accuracy of the chip is ±0.4℃.

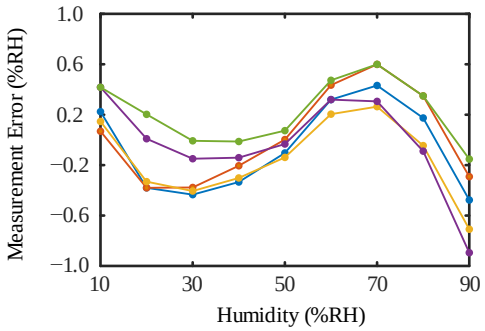

Fig. 11 Errors of humidity sensing

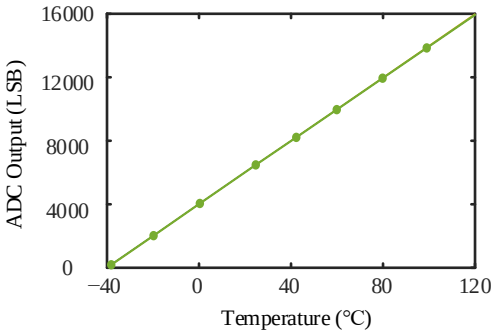

Fig. 12 Relationship between the ADC output and temperature

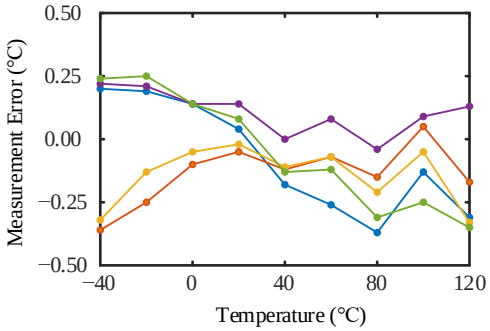

Fig. 13 Errors of temperature sensing

The key parameters of our design are compared with the published results of T/H sensors, shown in Table I. It can be seen that the integrated T/H sensor designed in this paper has certain advantages in temperature and humidity measurement accuracy.

Table I. Parameters comparison

Parameter	This work	[30]	[3]	SHT15
Process(nm)	153	180	180	-
Supply Voltage(V)	3.3	1.5~2	1.55	2.4~5.5
Power(μW)	1980*	15.6	3875	3000
Measurement range(%RH)	10~90	10~95	0~100	0~100
RH accuracy (%RH)	−0.9~0.6	±1.1	±2.0	±4.0
RH resolution (%RH)	0.03	0.007	0.006	0.05
Measurement range(℃)	−40~120	−40~85	−20~85	−40~120
Temp accuracy (℃)	±0.4	±0.25	±0.3	±1.5
Temp resolution (℃)	0.01	0.015	0.002	0.01

* The conversion current is 600μA.

6. Conclusion

In summary, we designed an integrated T/H sensor with a new sampling architecture. The T/H measurement is integrated on one chip, i.e. the T/H sensing probe is combined with one ΣΔ ADC. ADC selects a reasonable reference voltage according to varied range of different signals. Therefore, the dynamic range utilization rate of ADC is improved. The sensor is designed and fabricated in 0.153μm CMOS technology. The experimental results show that the temperature and humidity measurement accuracy are ±0.4℃ (@−40~120℃) and −0.9~0.6%RH (@10~90%RH), respectively.

References

[1] J. Jun, S. Shin, M. Kim, Y. Ahn and S. Kim: "A ±0.15% RH Inaccuracy Humidity Sensing System With ±0.44 °C (3σ) Inaccuracy On-Chip Temperature Sensor," IEEE Sensors Journal

21 (2021) 2115 (doi: 10.1109/JSEN.2020.3017508).
[2] Fang zhen, Wu Yu, Zhao Zhan, et al: “Research on Integrated Temperature and Humidity Sensor Based on MEMS,” Chinese Journal of Scientific Instrument **S2** (2004) 123 (in Chinese)(doi: 10.3321/j.issn:0254-3087.2004.z3.041).
[3] M. Maruyama, S. Taguchi, M. Yamanoue and K. Iizuka: "An Analog Front-End for a Multifunction Sensor Employing a Weak-Inversion Biasing Technique With 26 nVrms, 25 aCrms, and 19 fArms Input-Referred Noise," IEEE J. Solid-State Circuits **51** (2016) 2252 (doi: 10.1109/JSSC.2016.2581812).
[4] Eder C, Valente V, Donaldson N, et al: “A CMOS Smart Temperature and Humidity Sensor with Combined Readout,” Sensors **14** (2014) 17192 (doi: 10.3390/s140917192).
[5] Y. He, X. Zhang, H. Zhang and Z. Lin: "Design and Implementation of Intelligent Temperature and Humidity Control System for Small and Medium Grain Depots," ICSGEA (2021) 101 (doi: 10.1109/ICSGEA53208.2021.00028).
[6] Y. Wang, et al: “A 9 μW micropower temperature sensor with an inaccuracy of ±0.4°C from −40°C to 120°C,” Nanosci. Nanotechnol. Lett. **6** (2014) 898.
[7] B. Yousefzadeh, S. Heidary Shalmany and K. A. A. Makinwa: "A BJT-Based Temperature-to-Digital Converter With ±60 mK (3 σ) Inaccuracy From −55 °C to +125 °C in 0.16-μm CMOS," IEEE J. Solid-State Circuits **52** (2017) 1044 (doi: 10.1109/JSSC.2016.2638464).
[8] K. Souri, Y. Chae and K. A. A. Makinwa: "A CMOS Temperature Sensor With a Voltage-Calibrated Inaccuracy of ± 0.15°C (3σ) From −55°C to 125°C," in IEEE Journal of Solid-State Circuits **48** (2013) 292 (doi: 10.1109/JSSC.2012.2214831).
[9] T. Someya, V. van Hoek, J. Angevare, S. Pan and K. Makinwa: "A 210 nW NPN-Based Temperature Sensor With an Inaccuracy of ±0.15 °C (3σ) From −15 °C to 85 °C Utilizing Dual-Mode Frontend," IEEE Solid-State Circuits Letters **5** (2022) 272 (doi: 10.1109/LSSC.2022.3222578).
[10] R. K. Kumar, H. Jiang and K. A. A. Makinwa: "An Energy-Efficient BJT-Based Temperature-to-Digital Converter with ±0.13°C (3σ) Inaccuracy from -40 to 125°C," A-SSCC (2019) 107 (doi: 10.1109/A-SSCC47793.2019.9056962).
[11] J. A. Angevare, Y. Chae and K. A. A. Makinwa: "A Highly Digital 2210μm2 Resistor-Based Temperature Sensor with a 1-Point Trimmed Inaccuracy of ± 1.3°C (3 σ) from -55°C to 125°C in 65nm CMOS," ISSCC (2021) 76 (doi: 10.1109/ISSCC42613.2021.9365995).
[12] S. Pan and K. A. A. Makinwa: "3.6 A CMOS Resistor-Based Temperature Sensor with a 10fJ·K2 Resolution FoM and 0.4°C (30) Inaccuracy From −55°C to 125°C After a 1-point Trim," ISSCC (2020) 68 (doi: 10.1109/ISSCC19947.2020.9063064).
[13] K. Yang et al.: "9.2 A 0.6nJ −0.22/+0.19°C inaccuracy temperature sensor using exponential subthreshold oscillation dependence," ISSCC (2017) 160 (doi: 10.1109/ISSCC.2017.7870310).
[14] D. S. Truesdell and B. H. Calhoun: "A 640 pW 22 pJ/sample Gate Leakage-Based Digital CMOS Temperature Sensor with 0.25°C Resolution," CICC (2019) 1 (doi: 10.1109/CICC.2019.8780382).
[15] X. Wang, P. -H. P. Wang, Y. Cao and P. P. Mercier: "A 0.6V 75nW All-CMOS Temperature Sensor With 1.67m°C/mV Supply Sensitivity," IEEE Trans. Circuits Syst. I, Reg. Papers **64** (2017) 2274 (doi: 10.1109/TCSI.2017.2707325).
[16] Zhou C, Zhang X, Tang N, et al: “Rapid response flexible humidity sensor for respiration monitoring using nano-confined strategy,” Nanotechnology **31**(2020) 125302 (doi: 10.1088/1361-6528/ab5cda).
[17] Xu Yanyan, Li Jun, Li Hao, et al: “Research on Humidity Sensor Based on Tapered Seven Core Fiber,” Chinese Journal of Lasers **48** (2021) 1(in Chinese).
[18] N. Saeidi, J. Strutwolf, A. Maréchal, A. Demosthenous and N. Donaldson: "A Capacitive Humidity Sensor Suitable for CMOS Integration," IEEE Sensors Journal **13** (2013) 4487 (doi: 10.1109/JSEN.2013.2270105).
[19] H. Li et al.: "Energy-Efficient CMOS Humidity Sensors Using Adaptive Range-Shift Zoom CDC and Power-Aware Floating Inverter Amplifier Array," IEEE J. Solid-State Circuits **56** (2021) 3560 (doi: 10.1109/JSSC.2021.3114189).
[20] Z. Tan, R. Daamen, A. Humbert, Y. V. Ponomarev, Y. Chae and M. A. P. Pertijs: "A 1.2-V 8.3-nJ CMOS Humidity Sensor for RFID Applications," IEEE J. Solid-State Circuits **48** (2013) 2469 (doi: 10.1109/JSSC.2013.2275661).
[21] M. A. P. Pertijs, A. Bakker and J. H. Huijsing: "A second-order sigma-delta ADC using MOS capacitors for smart sensor applications [smart temperature sensor]," SENSORS (2004) 421 (doi: 10.1109/ICSENS.2004.1426189).
[22] Y. Zhao et al.: "A 94.1 dB DR 4.1 nW/Hz Bandwidth/Power Scalable DTDSM for IoT Sensing Applications Based on Swing-Enhanced Floating Inverter Amplifiers," CICC (2021) 1 (doi: 10.1109/CICC51472.2021.9431415).
[23] S. Park, G. -H. Lee and S. Cho: "A 2.92-μW Capacitance-to-Digital Converter With Differential Bondwire Accelerometer, On-Chip Air Pressure, and Humidity Sensor in 0.18-μm CMOS," IEEE J. Solid-State Circuits **54** (2019) 2845 (doi: 10.1109/JSSC.2019.2930140).
[24] A. Bakker: "CMOS smart temperature sensors - an overview," SENSORS **2** 1423 (doi: 10.1109/ICSENS.2002.1037330).
[25] M. A. P. Pertijs and J. H. Huijsing: *Precision Temperature Sensor in CMOS Technology* (Springer, Netherlands, 2006) (DOI: 10.1007/1-4020-5258-8_1).
[26] M. A. P. Pertijs, K. A. A. Makinwa and J. H. Huijsing: "A CMOS smart temperature sensor with a 3σ inaccuracy of ±0.1 °C from -55 °C to 125 °C," IEEE J. Solid-State Circuits **40** (2005) 2805 (doi: 10.1109/JSSC.2005.858476).
[27] Zhu Zilan, Li Wenchang, Yang Wenxuan, et al: “A Programmable Capacitance-Voltage Converter,” Microelectronics **51** (2021) 5 (in Chinese) (doi: 10.13911/j.cnki.1004-3365.200076).
[28] R. Schreier and G. C. Temes: *Understanding Delta-Sigma Data Converters*. New York, NY, USA: Wiley, 2004.
[29] B. Razavi: *Design of Analog CMOS Integrated Circuits* (McGraw-Hill, New York, 2001)
[30] H. Jiang, C. -C. Huang, M. R. Chan and D. A. Hall: "A 2-in-1 Temperature and Humidity Sensor With a Single FLL Wheatstone-Bridge Front-End," IEEE J. Solid-State Circuits **55** (2020) 2174 (doi: 10.1109/JSSC.2020.2989585).